

## ORIGINAL ARTICLE

# Overexpression of BCCIP predicts an unfavorable prognosis and promotes the proliferation and migration of lung adenocarcinoma

Jie Shi  | Xin Lv | Wei Li  | Zongjuan Ming | Lizhong Zeng | Jingyan Yuan | Yang Chen | Boxuan Liu | Shuanying Yang

Department of Pulmonary and Critical Care Medicine, The Second Affiliated Hospital of Xi'an Jiaotong University, Xi'an, China

**Correspondence**

Shuanying Yang, Department of Pulmonary and Critical Care Medicine, The Second Affiliated Hospital of Xi'an Jiaotong University, 157th Xi wu Road, Xi'an, China.  
Email: yangshuanying@xjtu.edu.cn

**Funding information**

Data Center of Management Science, National Natural Science Foundation of China - Peking University, Grant/Award Number: 81672300; free exploration and innovation project of Xi'an Jiaotong University, Grant/Award Number: xjj2018144

**Abstract**

**Background:** Lung cancer accounts for the highest rate of cancer-related diagnosis and mortality. Lung adenocarcinoma (LUAD) is the most common histopathological type. BCCIP was originally identified as a BRCA2 and CDKN1A interacting protein. In different cancers, BCCIP plays different roles. The role of BCCIP in LUAD is still unknown.

**Methods:** The expression and prognostic value of BCCIP was analyzed using public databases, including LCE, GEPIA, TCGA, and clinical specimens. Bioinformatic analysis and vitro experiments were conducted to explore the biological functions of BCCIP in LUAD. By using the GEPIA and TIMER databases, we investigated the correlations between LUAD expression and immune infiltration in LUAD.

**Results:** Compared with normal tissue, LUAD tissue had a higher expression level of BCCIP and high expression level of BCCIP was detrimental to LUAD patient survival. The suppression of BCCIP inhibited LUAD cell proliferation, migration and resulted in G1/S phase arrest in vitro. Bioinformatic analysis demonstrated that BCCIP could be associated with cell cycle, DNA repair and E2F transcription factor family. There were significant correlations between BCCIP expression and immune infiltrates, including B cell, CD4+ T cell, macrophage, neutrophil and dendritic cells. Furthermore, BCCIP expression showed strong correlations with diverse immune marker sets in LUAD, such as B cell, macrophage and DC.

**Conclusions:** Overexpression of BCCIP predicts an unfavorable prognosis and promotes the proliferation and migration of lung adenocarcinoma cells. BCCIP is correlated with immune infiltration in LUAD. Suppression of BCCIP may be a potential approach in the prevention and treatment of LUAD.

**KEYWORDS**

BCCIP, immune infiltration, lung adenocarcinoma, migration, proliferation, tumor microenvironment

## INTRODUCTION

Lung cancer, primarily non-small cell lung cancer (NSCLC), accounts for the highest incidence and cancer-linked morbidity globally.<sup>1</sup> In NSCLC, lung adenocarcinoma (LUAD) constitutes the most frequent histopathological type. Despite great advances in its diagnosis and treatment, such as targeted therapies and immune checkpoint inhibitors (ICIs),

the average 5-year survival rate for LUAD is approximately 19%<sup>2</sup> and has not improved in recent decades.<sup>3</sup> Hence, a profound comprehension of the molecular mechanisms of LUAD, which further aggravates effective treatment, has become an area of keen interest.

In human cells, the BCCIP gene, initially recognized as a BRCA2 and CDKN1A cross talking protein, has two distinct transcripts coding for BCCIP $\alpha$  (consisting of 322 amino

acids), as well as BCCIP $\beta$  (with 314 amino acids).<sup>4,5</sup> Both isoforms have the same domain sequences in the N-terminus acidic domain (NAD), internal conserved domain (ICD), thus, the two isoforms may have a similar function. The critical roles of BCCIP in HR-dependent DNA repair,<sup>6</sup> to regulate RAD51 and p53,<sup>7,8</sup> facilitate G1/S and mitotic cell cycle transitions<sup>9,10</sup> maintain centrosome and spindle cell fidelity,<sup>11</sup> and regulate ribosomal proteins<sup>12</sup> have already been reported in multiple studies. The loss of BCCIP has been previously reported to cause medulloblastoma in mice.<sup>13</sup> The known BCCIP mechanisms indicate that BCCIP may be a tumor suppressor gene. BCCIP dysregulation has been verified in hepatocellular carcinoma,<sup>14</sup> colorectal cancer and renal cell carcinoma tissue.<sup>15</sup> Nevertheless, there are studies which suggest that BCCIP might promote tumor progression. In esophageal squamous cell carcinoma, BCCIP  $\beta$  constitutes an oncogene which has been reported to amount to a dismal patient outcome.<sup>16</sup> The role of BCCIP in LUAD remains largely unknown.

In data from patients with LUAD in various public databases, including The Cancer Genome Atlas (TCGA), we found BCCIP expression was remarkably elevated in LUAD tissue relative to healthy tissue and verified by clinical immunohistochemistry. The patients with elevated BCCIP expression had remarkably shorter overall survival. In vitro, BCCIP promotes cell proliferation and migration. Using multidimensional analysis, we explored the BCCIP-regulated functional networks in LUAD and investigated its function in tumor immunity. Our study has revealed potential targets for LUAD diagnosis and treatment.

## METHODS

### LCE database analysis

LCE (The Lung Cancer Explorer) repository (<http://lce.biohpc.swmed.edu/>) constitutes a lung

cancer-distinct repository that includes gene expression data, as well as clinical data involving over 6700 patients in 56 studies.<sup>17</sup> LCE provides the meta-analysis differential expression between lung cancer and normal samples.

### GEPIA database assessment

The Gene Expression Profiling Interactive Analysis database (GEPIA) (<http://gepiacancer-pku.cn/>) is a database including 9736 tumors, as well as 8587 normal samples from TCGA and the GTEx projects.<sup>18</sup> GEPIA was employed to explore the differential expression of mRNA between tumor and normal samples.

### LinkedOmics database evaluation

LinkedOmics repository (<http://www.linkedomics.org/login.php>) is a web-centered resource for evaluating 32

multidimensional datasets of TCGA, which are cancer-linked.<sup>19</sup> The co-expression of the BCCIP gene was statistically examined via correlation coefficient, and the data presented using volcano diagrams and heatmaps. We inspected the function module of transcription factor-target enrichment, kinase-target enrichment and miRNA-target enrichment via gene set enrichment analysis (GSEA). The rank criterion consisted of FDR <0.05, with 1000 simulations conducted.

### Metascape database assessments

The Metascape repository (<http://metascape.org/gp/index.htm>) constitutes a web-based bioinformatic workflow for multiple list of genes that shows effective decisions of gene prioritization that is data-centered.<sup>20</sup> The generic evaluation pipeline entailed mining gene list annotations via gene ontology (GO) biological processes as well as pathways and functional enrichment assessment. The remaining terms which were significant were then classified in a hierarchical manner to form a tree hinged on Kappa-statistical similarities among the membership of their genes. We employed a kappa score of 0.3 as the threshold to cast the tree into term clusters.

### TIMER database analysis

The tumor immune estimation resource (TIMER) database (<https://cistrome.shinyapps.io/timer/>) is an exhaustive web resource for the systematic inspection of immune infiltrates from TCGA, which includes 10 897 malignancy samples across 32 kinds of cancer.<sup>21</sup> From gene expression patterns, TIMER employs a deconvolution approach<sup>22</sup> to deduce the abundance of tumor-infiltrating immune cells (TIICs).<sup>22</sup>

### Survival analysis

Raw counts of RNA-sequencing data (level 3) and corresponding clinical information were obtained from TCGA and Gene Expression Omnibus (GEO) dataset, in which the method of acquisition and application complied with the guidelines and policies. For Kaplan–Meier curves, *p*-values and hazard ratio (HR) with 95% confidence interval (CI) were generated by log-rank tests and univariate Cox proportional hazards regression. All analytical methods described above and R packages were performed using R software version v4.0.3 (The R Foundation for Statistical Computing, 2020). *p* < 0.05 was considered statistically significant.

### Cell lines and tissue specimens

BEAS-2B, SKMES1, PC9, 95C, 95D, H520, A549 and H1299 cells were acquired from American Type Culture Collection (Manassas, VA). The tissue donation program was approved

by the Ethical Committee of the second affiliated hospital of Xi'an Jiaotong University. LUAD and adjacent normal tissue were acquired by biopsy or surgical procedures from 52 patients at the second affiliated hospital of Xi'an Jiaotong University. All patients had histologically confirmed LUAD. Clinical staging, including stage I, II, III and IV, was established as per the tumor node metastasis (TNM) categorization of the Chinese Society of Clinical Oncology.

### Lentivirus vectors for BCCIP small interfering RNA

PGCL-GFP-lentivirus was employed in expressing the small interfering RNAs (siRNAs) that targeted BCCIP. A nontargeting sequence was employed as a lentivirus negative control (NC) and acquired from Shanghai Genechem, Co. Ltd. The RNA interference target sequence was 5'-TTCTGATTAGTAAGACATT-3'. The sequences were cloned into the pGCSIL-GFP (GeneChem) to create the lentiviral vectors.

### Infection of cells with BCCIP-siRNA lentivirus

A549 and H1299 cells were infected with BCCIP-siRNA lentivirus, as well as NC lentivirus. No transfected cells were treated as a control. Following three days of infection, fluorescent microscopy was used to obtain GFP expression. Following five days of infection, cells were harvested to inspect silencing efficiency via qRT-PCR.

### Cell growth assay

A549 and H1299 cells with either NC or BCCIP siRNA lentivirus were planted at 2000 cells per well in 96-well dish plates, then incubated at 37°C with 5% CO<sub>2</sub> for five days. Dish-plates were processed with the Celigo image cytometer (Nexcelom Inc.) each day. The cytometer is a computerized, automated fluorescence-imaging microscope that automatically identifies stained cells and reports the intensity and distribution of fluorescence in each individual cell.

### RNA preparation and qRT-PCR

Total RNA from whole-cells lysates were purified using TRIzol (Life Technologies). Generation of cDNA was done using the PrimeScript RT Master Mix (Takara) from 500 ng of RNA to quantify the amount of mRNA. SYBR Premix Ex Taq II (Takara) was employed for qRT-PCR analyses.

### Protein preparation and western blotting

Homogenization of the cells for 30 min in the lysis buffer on ice (50 mM Hepes, 5 mM EDTA, 150 mM NaCl, 50 mM

NaF, 20 mM  $\beta$ -glycerophosphate, 1 mM dithiothreitol [DTT] and protease inhibitor cocktail [Roche]) was done. Centrifugation of the lysates for 10 min at 4°C was done to clarify them. Proteins (25  $\mu$ g/lane) were fractionated on 10% SDS-polyacrylamide gels and transfer-embedded onto nitrocellulose membranes. Rabbit polyclonal anti-mTOR (CST), anti-MYC (Abcam), anti-CDK1 (Abcam), anti-FOXM1 (Abcam), anti-CCNB1 (Sigma), anti-E2F6 (Abcam) and mouse monoclonal anti-GAPDH (Santa-Cruz) were used in immunoblots. Immunostained bands were developed and detected by the chemiluminescent method.

### Immunohistochemistry (IHC)

Paraffin segments were conjugated with primary antibodies against BCCIP (1:800) (Abcam) via overnight incubation at 4°C. After that, secondary antibodies were conjugated at 37°C for 1 h, and then labeling with HRP-conjugated streptavidin solution for 10 min and staining with diaminobenzidine (DAB) was conducted.

### Oris wound-healing assay

A confluent monolayer of A549 and H1299 cells were cultured on 96-wells with Oris stopper barriers overnight which were subsequently carefully removed. Images were then captured at 24 and 48 h using a Celigo image cytometer (Nexcelom).

### MTT

A549 and H1299 cells were cultured on 96-wells petri dishes. Then, 0.5 ng/ml MTT solution was introduced to each well at diverse time points (from 1 to 5 days). Incubation of the plates at 37°C for 4 h was performed. The consequent formazan crystals were liquefied by the addition of DMSO and absorbance was inspected at 560 nm. A microplate reader was employed to measure cell viability.

### Flow cytometry inspection of cell apoptosis

After A549 and H1299 cells were grown for 72 h and harvested, 10  $\mu$ l of Annexin V-APC (eBioscience) was added to each tube. Following incubation in the dark at RT for 20 min, we used a BD FACSCAN flow cytometer (Becton-Dickinson) to analyze the cells.

### Flow cytometry evaluation of cell cycle

We collected the A549 and H1299 cells which were fixed at 4°C in 70% ice-chilled ethanol for more than 24 h. They were subsequently washed three times with PBS, and



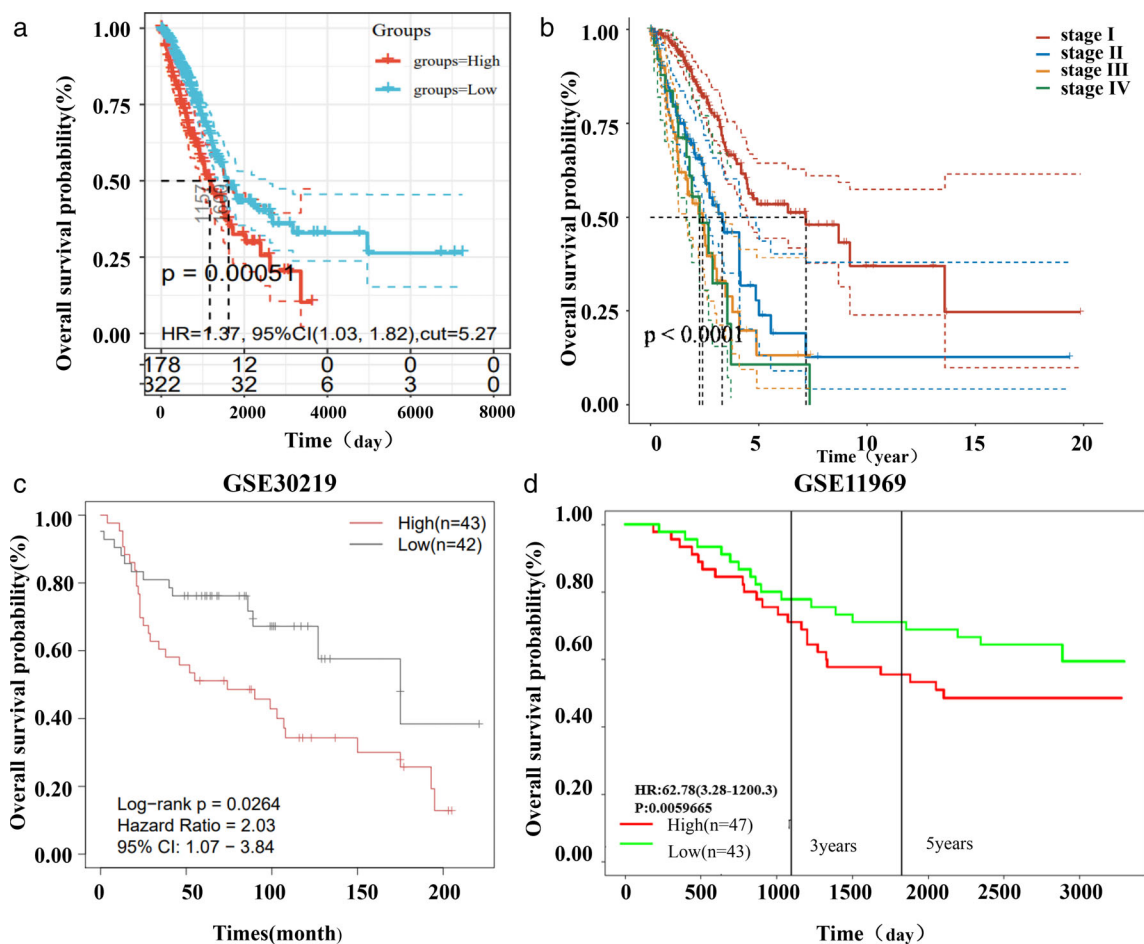


**FIGURE 2** BCCIP is associated with survival outcome in LUAD. (a) Kaplan–Meier survival analysis of BCCIP in LUAD from TCGA database. (b) Kaplan–Meier survival analysis of BCCIP in LUAD with different TNM stages from TCGA database. (c) Kaplan–Meier survival analysis of BCCIP in LUAD from the GSE30219 cohort. (d) Kaplan–Meier survival analysis of BCCIP in LUAD from the GSE11969 cohort

$p < 0.05$ ) relative to the low expression group (Figure 2 (c),(d)).

### Upregulation of BCCIP in LUAD samples

To investigate whether the expression of BCCIP was altered in LUAD, we first examined the expression of BCCIP in 52 pairs of LUAD tissues against the adjacent normal tissues using qRT-PCR (Figure 3(a)) and IHC (Figure 3(b)). Relative to the adjacent normal tissues, LUAD tissues showed increased expression of BCCIP. Similarly, the levels of BCCIP expression in lung cancer cell lines (H520, SKMES1, H226, 95C, 95D, A549 and PC9) were also increased relative to the healthy human bronchial epithelial cell line (BEAS-2B) (Figure 3(c)). To interrogate the relationship between BCCIP and patient prognosis, a cohort of 52 LUAD subjects with clinicopathological features, as well as survival data, was analyzed. We established that BCCIP expression was directly linked to tumor node metastasis stage (TNM) ( $p = 0.0234$ ), tumor size ( $p = 0.0276$ ) and lymph node

metastasis ( $p = 0.00314$ ), but not with other clinicopathological characteristics such as age, or gender (Table 1). In addition, LUAD subjects with lower BCCIP expression showed a better overall survival (log-rank  $p = 0.0242$ ) (Figure 3(d)). Collectively, these data opines that BCCIP was overexpressed in LUAD tissues and higher BCCIP expression led to a poor prognosis.

### BCCIP promotes cell proliferation and migratory in vitro

We further investigated the functional role of BCCIP in LUAD progression. We first blocked BCCIP expression in A549 and H1299 cells lines by transfection with BCCIP-siRNA lentivirus to decrease BCCIP expression level (Figure 4(a)). The results of cell growth assay and MTT assay indicated that silencing of BCCIP could repress cell proliferation in A549 and H1299 cells (Figure 4(b),(c)). Cell-cycle assays showed that silencing of BCCIP caused cell-cycle arrest in G1/S phase (Figure 4(d)). Meanwhile, cell

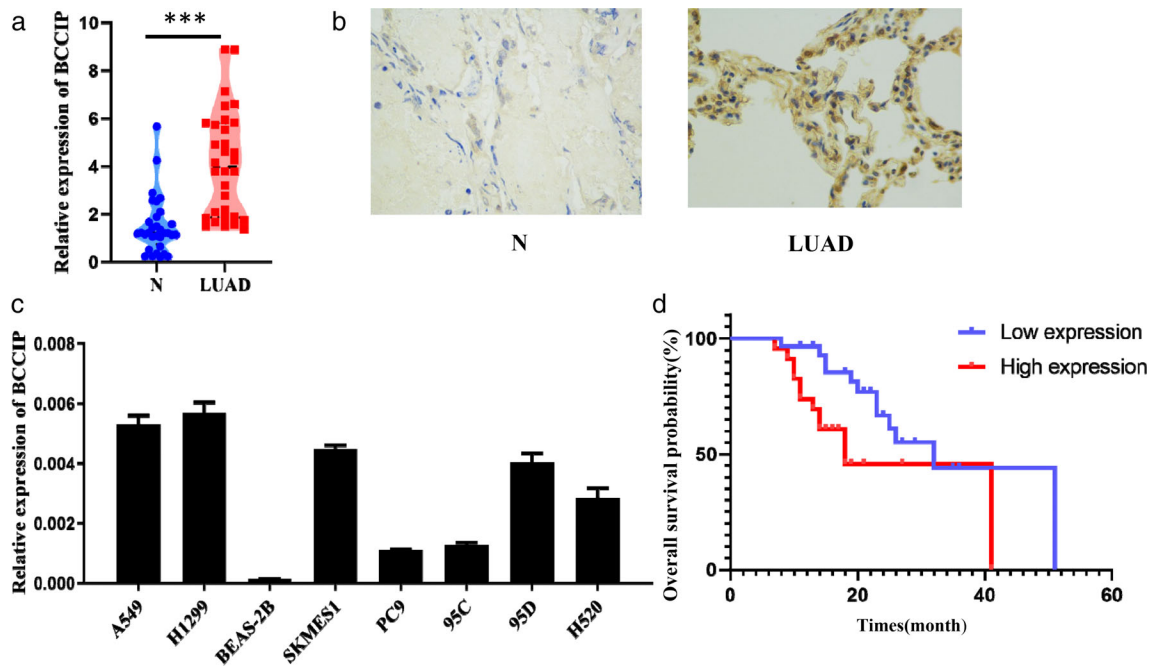


**FIGURE 3** BCCIP expression levels are increased in LUAD tissue and cell lines. (a) BCCIP mRNA levels in 52 LUAD tissues and the adjacent normal tissues. (b) Immunohistochemistry analysis of BCCIP in LUAD tissues and the adjacent normal tissues (400-fold magnification). (c) BCCIP mRNA levels in seven LUAD cell lines. (d) OS of BCCIP in 52 LUAD patients

**TABLE 1** Correlation between BCCIP expression and clinicopathological characteristics of LUAD patients ( $N = 52$ )

Characteristics	Total number	Low expression ( $N = 29$ )	High expression ( $N = 23$ )	$p$ -value
Age				0.3301
<60	21	10	11	
$\geq 60$	31	19	12	
Gender				0.6855
Male	31	18	13	
Female	21	11	10	
Smoking history				0.507
Yes	32	19	13	
No	20	10	10	
TNM stage				0.0234
I-II	25	18	7	
III-IV	27	11	16	
Tumor size				0.0276
$\leq 5$ cm	27	19	8	
$> 5$ cm	25	10	15	
Lymph node metastasis				0.0314
Yes	23	9	14	
No	29	20	9	

apoptotic was induced by knockdown of BCCIP as revealed by the Annexin-V assay (Figure 4(f)). Wound healing, and transwell migration data demonstrated that silencing of BCCIP diminished the migratory capabilities of A549 and H1299 cells (Figure 4(e),(g)). These data implied that decreased BCCIP reduced the proliferation and migration of A549 and H1299 cells.

### BCCIP co-expression networks in LUAD

The function module of LinkedOmics was employed to inspect BCCIP co-expression mode to explore the biological mechanism of BCCIP in LUAD. As a result, there were 3241 genes (dark red dots) which showed remarkably positive associations and 5000 genes (dark green dots) which showed

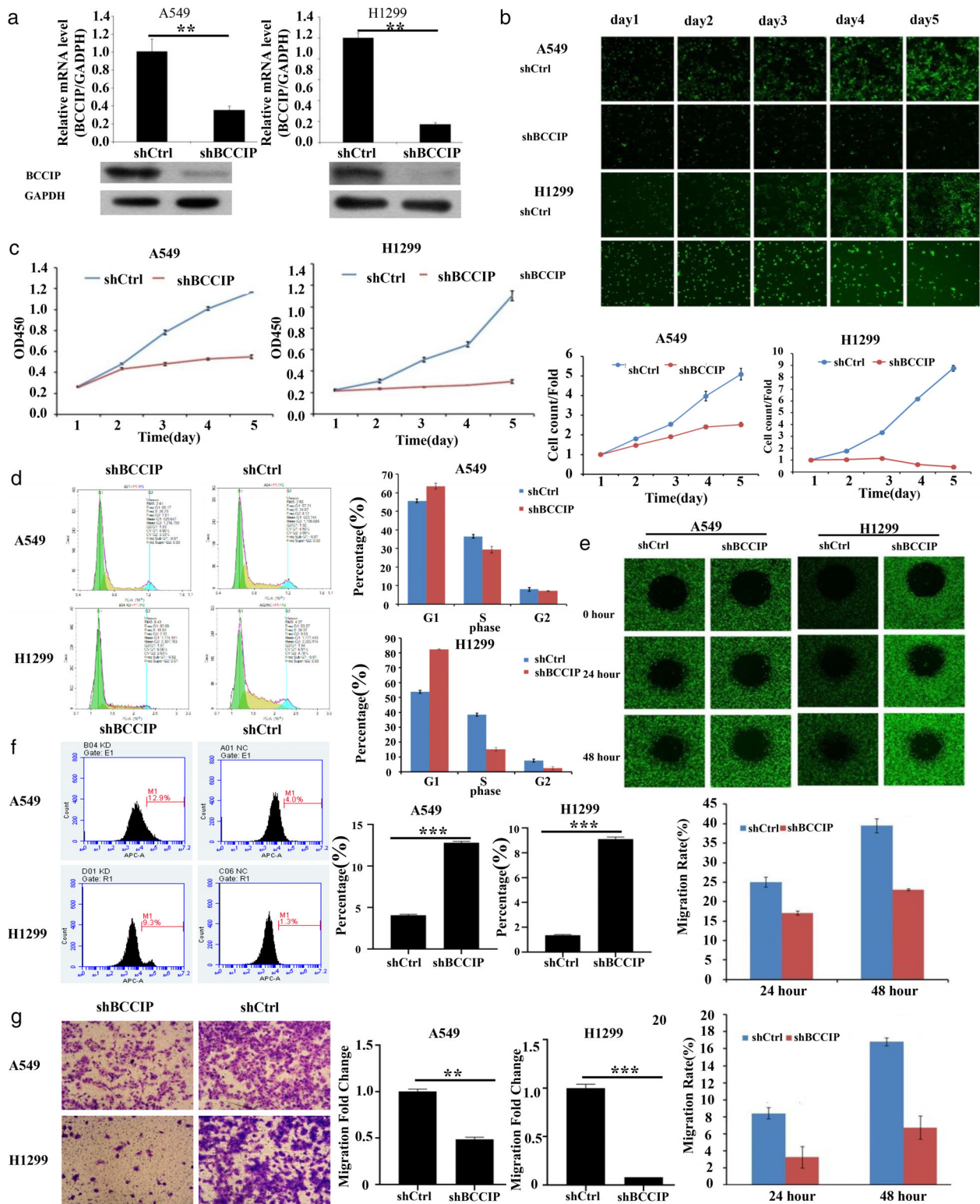


**FIGURE 4** The biological role of BCCIP in LUAD cell lines A549 and H1299. (a) RT-qPCR (up) and Western blot (down) assessment of BCCIP expression levels in H1299 and A549 cells after transfection with BCCIP-siRNA lentivirus. (b) Effect of BCCIP knockdown on cell growth (400-fold magnification). The rate of cell growth was monitored on the second, third, fourth and fifth days by assay ( $p < 0.05$ ). (c) Impact of BCCIP knockdown on cell proliferation. The shBCCIP group showed remarkably lower proliferation potential than the control group at third, fourth and fifth days ( $p < 0.05$ ). (d) Impact of BCCIP knockdown on cell cycle. (e) Impact of BCCIP silencing on cell migration by wound healing assays. Representative images are shown at 24 and 48 h after wound creation. Scale bar = 20  $\mu\text{m}$ . (f) The effect of BCCIP knockdown on cell apoptosis. (g) Impact of BCCIP silencing on cell migration by transwell migration. Images are shown at 72 h. scale bar = 20  $\mu\text{m}$ . Data are mean  $\pm$  SD,  $*p < 0.05$ ;  $**p < 0.01$ ;  $***p < 0.001$

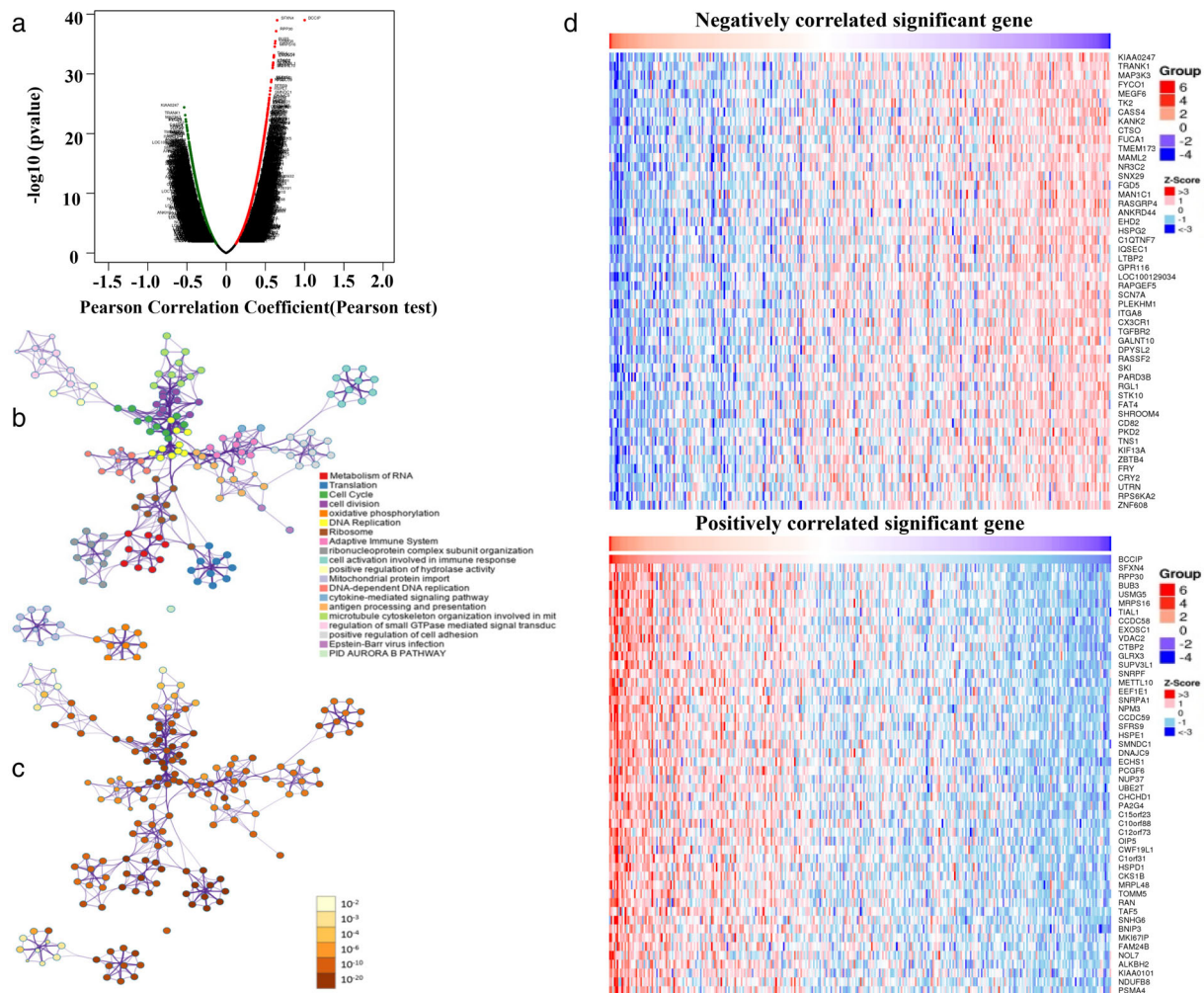


**FIGURE 5** BCCIP co-expression genes in LUAD (LinkedOmics). (a) The volcano map shows BCCIP highly associated genes in the LUAD cohort. Dark red dots are the genes that are remarkably positively associated with BCCIP and the dark green dots are the genes obviously negatively associated with BCCIP (FDR < 0.01). (b, c) Gene ontology (GO) biological process analysis on co-expressed genes with a correlation coefficient greater than 0.3 with BCCIP by cluster ID and *p*-value. A circle node denotes a term. The size of the node corresponds to the enumeration of input genes falling into the respective term, whereas the color of the node signifies the identity of the class to which it belongs. (d) Heat maps indicate the top 50 genes positively and negatively linked to BCCIP in LUAD. Red denotes positively linked genes and blue designates negatively linked genes

obviously negative relationships with BCCIP (FDR < 0.01) (Figure 5(a)). The top 50 distinct genes directly or inversely linked to BCCIP are shown in the heat map (Figure 5(d)).

The Metascape database was used to provide statistically enriched analysis for co-expressed genes with a correlation coefficient greater than 0.3. These subnetworks, which entailed clusters labeled as metabolism of RNA (R-HSA-8953854), translation (R-HSA-72766, GO:0006412), ribonucleoprotein complex biogenesis (GO:0022613), mitochondrial gene expression (GO:0140053) and cell cycle (R-HSA-1640170, GO:0044770), were comprised of terms emanating from genes (Figures 5(b),(c) and Supplementary Table S1).

## Regulators of BCCIP networks in LUAD

We evaluated the kinases, miRNAs, as well as transcription factor (TF) enrichment of BCCIP co-expressed genes to

further explore the regulators of BCCIP in LUAD (Table 2). The top five most remarkable kinases were the cyclin-dependent kinase 1 (CDK1), polo like kinase 1 (PLK1), Aurora kinase B (AURKB), ataxia telangiectasia and Rad3-related (ATR), and polo like kinase 3 (PLK3) (Table S2). Apart from PLK3, all of these kinase genes were remarkably excessively expressed in LUAD tissues. Moreover, all of these kinase genes, except PLK3 and ATR, were remarkably linked to the OS of LUAD patients (Supplementary Figure S1). The miRNA-target network was linked to (GAGCCTG) MIR-484, (TTTGCAC) MIR-19A, as well as MIR-19B, (TTGCACT) MIR-130A, MIR-301 and MIR-130B, (GCACTTT) MIR-17-5P, MIR-20A, MIR-106A, MIR-106B, MIR-20B and MIR-519D, (GACAATC) MIR-219, (GTGCCTT) MIR-506, (GTGCAAT) MIR-25, MIR-32, MIR-92, MIR-363 and MIR-367 (Table S3). The transcription factors were majorly associated with the E2F transcription factor family, entailing V \$E2F\_Q6, V \$E2F\_Q4, V \$E2F1\_Q6, V \$E2F\_Q2, V

**TABLE 2** The kinases, miRNAs and transcription factors-target networks of BCCIP in LUAD

Enriched category	Gene set	Leading edge Num	FDR
Kinase target	Kinase_CDK1	76	0.00E+00
	Kinase_PLK1	29	0.00E+00
	Kinase_AURKB	40	9.75E-04
	Kinase_ATR	23	2.56 E-03
	Kinase_PLK3	8	3.22 E-03
miRNA Target	GAGCCTG,MIR-484	45	0.00E+00
	TTTGAC,MIR-19A,MIR-19B	171	0.00E+00
	TTGCACT,MIR-130A,MIR-301,MIR-130B	142	0.00E+00
	GCACTTT,MIR-17-5P,MIR-20A,MIR-106A,MIR-106B, MIR-20B,MIR-519D	211	0.00E+00
	GACAATC,MIR-219	56	0.00E+00
Transcription factor	SCGGAAGY_V\$ELK1_02	354	0.00E+00
	V\$E2F_Q6	68	0.00E+00
	V\$ELK1_02	72	0.00E+00
	V\$E2F_Q4	66	0.00E+00
	GGAANCGGAANY_UNKNOWN	40	0.00E+00

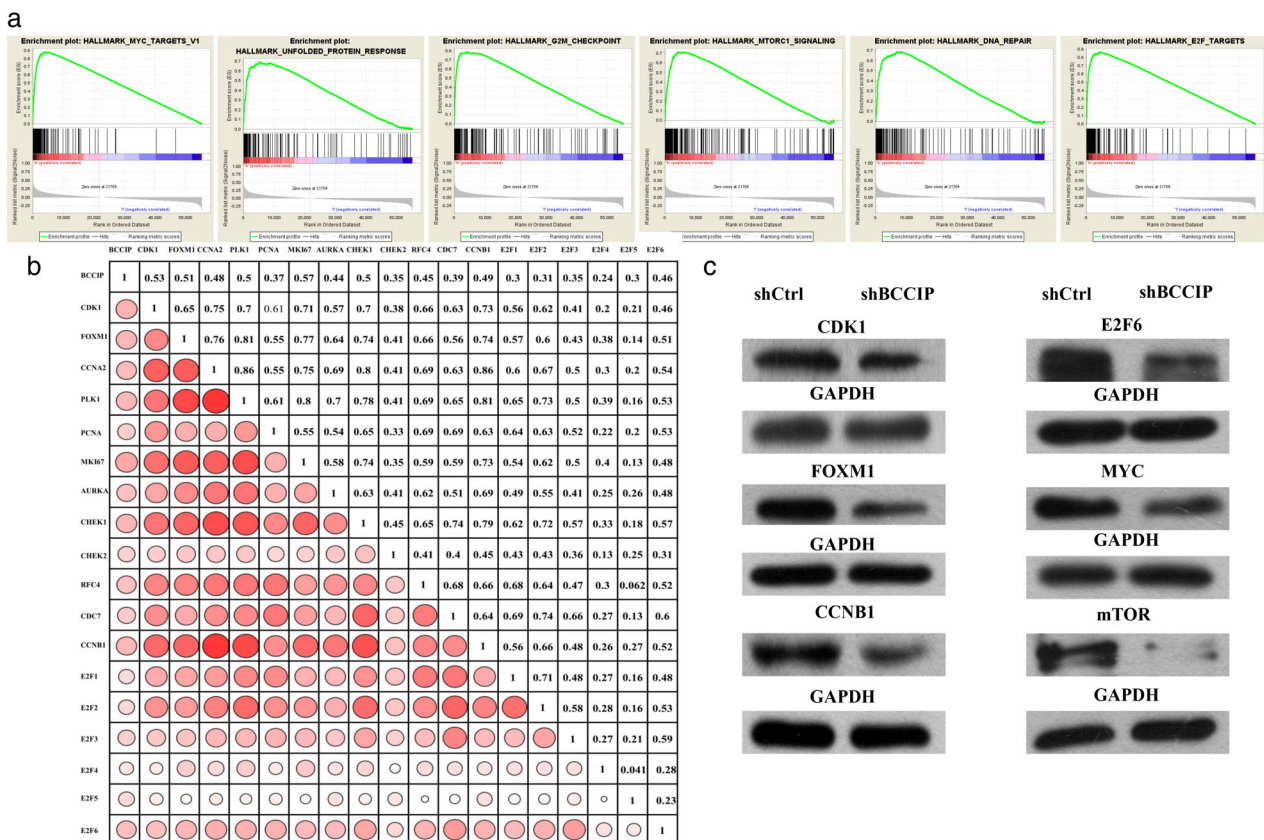


**FIGURE 6** BCCIP is linked to the cell cycle, DNA repair and E2F transcription factor family in LUAD. (a) GSEA of hallmarks pathway gene sets in BCCIP elevated expression compared with low expression samples from TCGA. Normalized enrichment score (NES), FDR and nominal *p*-value are indicated in each plot. (b). Correlation between BCCIP and cell cycle, DNA repair and E2F transcription factor family related molecules in LUAD samples from TCGA. (c) Western blot analysis of CDK1, FOXM1, CCNB1, E2F6, MYC and mTOR protein expression in A549 cells after transfection with BCCIP-siRNA lentivirus

\$E2F1DP1\_01\$, V\$E2F1DP2\_01\$, V\$E2F4DP2\_01\$ and V\$E2F4DP1\_01\$ (Table S4).

## Biological pathways of BCCIP in LUAD

GSEA analysis was performed to map into HALLMARK pathways database using 497 LUAD samples from TCGA database to inspect the biological role of BCCIP expression. Under the cutoff criteria, gene size  $\geq 20$ , FDR  $< 0.01$ , and enrichment score (ES)  $> 0.65$ , high expression BCCIP samples were enriched in MYC targets, unfolded protein response, MTORC1 signaling, E2F targets, DNA repair, oxidative phosphorylation and G2M checkpoint (Figure 6(a) and Supplementary Table S5). We noted that DNA repair, cell cycle and E2F family were all included in the results of BCCIP co-expression gene enriched terms and GESA, and therefore DNA repair, cell cycle and E2F family may be important BCCIP gene associated biological pathways.

Because of the core roles of key biomolecules in cell cycle modulation, DNA repair, as well as E2F transcription factor family in LUAD, we made a correlation analysis between BCCIP and several well-known genes from GEPIA. The results showed that BCCIP was highly related to CDK1, FOXM1 (Forkhead Box M1), CCNA2 (cyclin A2), PLK1, PCNA (proliferating cell nuclear antigen), MKI67 (bio-signature of proliferation Ki-67), AURKA, CHEK1 (checkpoint kinase 1), CHEK2 (checkpoint kinase 2), RFC4

(replication factor C subunit 4), CDC7 (cell division cycle 7), E2F1 (E2F transcription factor 1), E2F2 (E2F transcription factor 2), E2F3 (E2F transcription factor 3), E2F4 (E2F transcription factor 4), E2F5 (E2F transcription factor 5) and E2F6 (E2F transcription factor 6) (Figure 6(b)). In order to further verify the relationship between BCCIP and key-genes, we found that knockdown of BCCIP decreased CDK1, FOXM1, CCNB1, E2F6, MYC and mTOR expression remarkably (Figure 6(c)). As per these data, we surmised that BCCIP could modulate DNA repair, cell cycle and E2F family and serve a pivotal function during tumorigenesis in LUAD.

## BCCIP is linked to tumor purity and immune infiltration level in LUAD

GSEA analysis that mapped into the Gene Ontology database using 497 LUAD samples from TCGA database showed that low expression samples of BCCIP were enriched in macrophage activation, regulation of B cell receptor signaling cascade, positive modulation of CD4 positive alpha beta T cell activation and alpha beta T cell differentiation (Figure 7(a)). To confirm these results, we explored whether BCCIP expression was linked to immune infiltration levels in LUAD from TIMER database. The data revealed that BCCIP expression had a marked direct link to tumor purity ( $r = 0.139$ ,  $p = 1.89E-03$ ) and a remarkable inverse relationship with

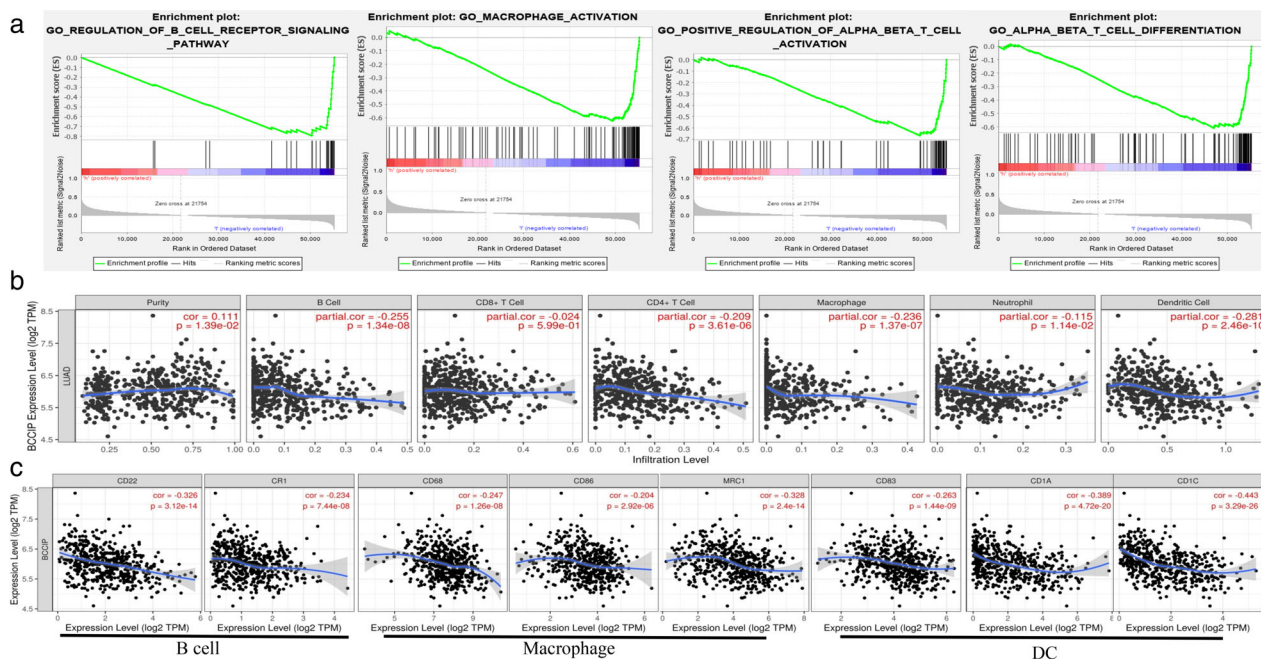


**FIGURE 7** The correlation of BCCIP expression with immune infiltration level in LUAD. (a) GSEA of GO pathway gene sets (biological process) in BCCIP high expression compared with low expression samples from TCGA. Normalized enrichment score (NES), FDR and nominal  $p$ -value are indicated in each plot. (b) BCCIP expression is remarkably directly associated with tumor purity, marked inverse associations with the levels of B cells, CD4 + T cells, dendritic cells, macrophages, as well as neutrophils. There is no association with CD8 + T cells. (c) BCCIP expression is correlated with B cell and DK infiltration, and macrophage polarization in LUAD. Markers include CD22 and CR1 of B cell, CD83, CD1A and CD1C of DK, and CD68, CD86 and MRC1 of TAM

TABLE 3 Correlations between BCCIP and gene markers of immune cells in LUAD

Cell type	Gene marker	None		Purity	
		Cor	p-value	Cor	p-value
B cell	CD19	-0.139	*	-0.098	*
	CD20	-0.182	***	-0.138	*
	CALLA	-0.115	*	-0.104	*
	CR1	-0.234	***	-0.205	***
	ENPP1	0.124	*	0.134	*
	CD22	-0.326	***	-0.308	***
	CR2	-0.128	*	-0.1	*
	CD38	-0.017	0.708	0.026	0.571
CD8+ T cell	CD8A	-0.019	0.662	0.034	0.454
	CD8B	-0.024	0.591	0.007	0.878
CD4+ T cell	CD4				
Tfh	CXCR5	-0.19	***	-0.148	**
	ICOS	-0.13	*	-0.085	0.0603
	CD200	-0.057	0.193	-0.022	0.619
	BTLA	-0.152	**	-0.103	*
	TNFRSF4	-0.17	**	-0.152	**
	SH2D1A	-0.108	*	-0.057	0.208
	BCL6	-0.026	0.0561	-0.018	0.697
	IL12R $\beta$ 2	0.223	***	0.264	***
Th1	IL27R	-0.257	***	-0.238	***
	STAT4	-0.167	**	-0.132	*
	TBX21	-0.106	*	-0.054	0.229
Th2	CCR3	-0.107	*	-0.076	0.0900
	STAT6	-0.112	*	-0.124	*
	GATA3	-0.129	*	-0.094	*
Th9	TGFBR2	-0.284	***	-0.262	***
	IRF4	-0.092	*	-0.041	0.363
	STAT5	-0.234	***	-0.204	***
	BATF	-0.151	**	-0.144	*
	TNF	-0.105	*	-0.055	0.221
Th17	IL21R	-0.16	**	-0.122	*
	IL6R	-0.176	***	-0.173	**
	IL23R	-0.069	0.12	-0.044	0.334
	STAT3	0.07	*	0.062	0.168
Th22	CCR10	0.061	0.167	0.045	0.323
	CCR6	-0.366	***	-0.357	***
	CCR4	-0.211	***	-0.186	***
	AHR	-0.25	***	-0.249	***
Treg	FOXP3	-0.142	*	0.127	*
	CCR8	-0.107	*	-0.077	0.0872
	Foxp3	-0.142	*	-0.12	*
	IL7R	-0.189	***	-0.153	**
	IL2RA	-0.056	0.208	-0.015	0.748
T cell exhaustion	PDCD1	-0.048	0.277	0.0006	0.89
	CTLA4	-0.075	0.0897	-0.021	0.637
Macrophage	CD68	-0.247	***	-0.224	***

(Continues)

TABLE 3 (Continued)

Cell type	Gene marker	None		Purity	
		Cor	p-value	Cor	p-value
M1	ITGAM	-0.326	***	-0.299	***
	SIGLEC1	-0.231	***	-0.214	***
	NOS2	0.006	0.896	0.015	0.733
	ROS1	-0.395	***	-0.386	***
M2	CD80	-0.203	***	-0.176	***
	ARG1	-0.065	0.142	-0.066	0.145
TAM	CD163	-0.14	*	-0.108	*
	HLA-G	-0.158	**	-0.123	*
	CD206				
	CD163	-0.14	*	-0.108	*
Monocytes	MRC1	-0.328	***	-0.311	***
	IRF3	-0.091	*	-0.077	0.0861
	CD86	-0.204	***	-0.177	***
	CD14	-0.217	***	-0.195	***
	CD16- FCGR3A	-0.099	*	-0.07	0.121
	CD43-SPN	-0.339	***	-0.32	***
NK	XCL1	0.101	*	0.111	*
	KIR3DL1	0.014	0.759	0.044	0.325
	CD2	-0.159	**	-0.118	*
	FCGR3A	-0.099	*	-0.07	0.121
Neutrophils	NCAM1	-0.047	0.285	-0.046	0.309
	CD7	0.007	0.872	0.051	0.259
	FUT4	-0.015	0.73	-0.003	0.941
	CD33	-0.381	***	-0.367	***
DC	MME	-0.115	*	-0.104	*
	MPO	-0.051	0.25	-0.02	0.654
	CD1C	-0.443	***	-0.428	***
	CD1A	-0.389	***	-0.376	***
	CD83	-0.263	***	-0.255	***
	THBD	-0.184	***	-0.165	**

Abbreviations: Cor, R value of Spearman's correlation; DC, dendritic cells; LUAD, lung adenocarcinoma; NK, natural killer cell; None, correlation without adjustment; TAM, tumor-associated macrophage; Tfh, follicular helper T cell; Th, T helper cell; Treg, regulatory T cell; Purity, correlation adjusted by for tumor purity.

\* $p < 0.05$ ; \*\* $p < 0.001$ ; \*\*\* $p < 0.0001$ .

invading B cell levels ( $r = -0.289$ ,  $p = 9.55E-03$ ), CD4+ T cell ( $r = -0.371$ ,  $p = 2.98E-17$ ), macrophage ( $r = -0.35$ ,  $p = 2.10E-15$ ), neutrophil ( $r = -0.274$ ,  $p = 9.42E-10$ ), as well as dendritic cells ( $r = -0.41$ ,  $p = 3.06E-21$ ) and no link to invading levels of CD8+ T cell (Figure 7(b)).

We then investigated the associations linking BCCIP and multiple immune cell markers in TIMER and GEPIA database (Table 3). These markers were employed in characterizing immune cells. After adjusting for tumor purity, the BCCIP expression was remarkably linked to 45 out of 73 immune cell markers in TIMER, which were mainly B cell, DC and macrophage markers. Moreover, we examined the relationships of BCCIP expression and B cell, DC and macrophage markers in the GEPIA (Table 4) and TIMER databases (Figure 7(c)). The data revealed that BCCIP is

correlated with Th1, Th9, Th22 and monocyte, especially with B cells, DC and macrophage markers in LUAD.<sup>22,23</sup>

## DISCUSSION

BRCA2 and CDKN1A-interacting protein is a protein encoded by the BCCIP gene. It is very important for cell viability and the maintenance of genomic stability. However, the role of BCCIP in cancer is still confusing. The known BCCIP mechanisms imply that BCCIP is a tumor repressor gene, but in esophageal squamous cell carcinoma, high expression of BCCIP  $\beta$  has been reported to promote tumor cell proliferation.<sup>16</sup> Recently, BCCIP has been shown to represent a paradoxical class of modulators for tumorigenesis

**TABLE 4** Correlations between BCCIP and genes markers of B cell, macrophage and DC in GEPIA

Cell type	Gene marker	Tumor		Normal	
		R	<i>p</i> -value	R	<i>p</i> -value
B cell	CD19	-0.21	***	-0.07	0.23
	MS4A1	-0.19	***	-0.26	***
	MME	0.089	0.051	-0.2	**
	CR1	-0.14	*	0.36	***
	ENPP1	0.124	*	0.024	0.68
	CD22	-0.26	***	0.06	0.31
	CR2	-0.12	*	0.035	0.56
	CD38	0.07	0.12	0.26	***
Macrophage	CD68	-0.16	**	0.23	***
	MRC1	-0.18	***	0.15	0.013
	ITGAM	-0.2	***	0.45	***
	SIGLEC1	-0.17	**	0.2	**
M1	NOS2	0.061	0.18	-0.15	0.012
	ROS1	-0.17	**	0.21	**
	CD80	-0.14	*	-0.066	0.26
M2	ARG1	0.023	0.61	0.073	0.22
	CD163	-0.082	0.073	0.33	***
TAM	HLA-G	-0.0051	0.91	0.24	***
	IRF3	-0.099	0.03	-0.17	*
	CD86	-0.17	**	-0.11	0.057
DC	CD1C	-0.25	***	-0.034	0.56
	CD1A	-0.14	*	-0.042	0.48
	CD83	-0.15	**	-0.21	**
	THBD	-0.025	0.59	0.11	0.059

\* $P < 0.05$ ; \*\* $P < 0.001$ ; \*\*\* $P < 0.0001$ .

as a suppressor for initiation but a requisite for progression (SIRP). So far, there has been no research which has explored the relationship between BCCIP and lung cancer. To gain profound comprehension into the prospective roles and biological mechanism of BCCIP in LUAD, we conducted bioinformatic analyses of public data and conducted a preliminary verification in order to assist the future research in LUAD.

In this study, high expression of BCCIP was observed in LUAD tissues relative to normal tissues using a public database. As verified, elevated protein and RNA expression of BCCIP were found in 52 LUAD tissues relative to normal tissues. These data implied that BCCIP expression is upmodulated in LUAD. Usually, an overexpressed gene in cancer tissues serves as a negative prognostic index and an oncogene. In LUAD, elevated BCCIP expression has been confirmed to be a dismal prognostic parameter. In vitro, BCCIP promotes cancer cell proliferation and migration, consistent with the upregulated expression of BCCIP in LUAD. Therefore, our data found that elevated BCCIP occurs in numerous cases of LUAD and requires further clinical confirmation as a promising diagnostic, as well as a prognostic biomarker.

To explore further the function of BCCIP in LUAD, a gene co-expression network was generated. Enrichment analysis of a highly related gene set of BCCIP using GSEA was employed to understand the significant networks of target kinases, miRNAs and transcription factors. We established that BCCIP in LUAD is linked to a network of kinases consisting of CDK1, PLK1, AURKB, ATR, and PLK3. CDK1 play an important role in the differentiation, modulation of mitosis, somatic reprogramming and self-renewal. Multiple repressors of CDK1 have been designed and some are in phase I or II clinical trials for the treatment of tumors.<sup>24</sup> Patients with increased CDK1 expression might indicate an increased incidence of cancer relapse and dismal survival in LUAD. AURKB is a key regulator of mitosis and the overexpression of AURKB has been observed in many solid tumors including lung cancer, which are also important KRAS targets in lung cancer.<sup>25</sup> ATR is a key kinase that senses replication stress (RS), DNA damage response (DDR) and signals to S and G2/M checkpoints to promote repair. Various inhibitors of ATR have been developed and four selective ATR inhibitors are currently in clinical development.<sup>26</sup> Polo-like kinases (PLKs) are pivotal players of

mitotic progression. PLKs, especially PLK1, have been thoroughly investigated as biomarkers and prospective treatment targets in oncology.<sup>27</sup> In LUAD, BCCIP might modulate DNA damage response and progression of the cell cycle through the cross talking of kinases.

The E2F family constitutes the main transcription factors for BCCIP. The family of E2F transcription factors is the key component of the CDK-RB-E2F axis, which is frequently inactivated in cancer. E2F modulates diverse cellular function linked to the cell cycle, as well as apoptosis and directly influences a number of biological processes through binding to thousands of genes.<sup>27</sup> The E2F1/2/3/5/6/7/8 expression has been previously reported to be elevated in LUAD, with high expression of E2F1/2/4/5/7/8 linked to low relapse-free survival (RFS) and high expression of E2F3/6 estimates elevating RFS in LUAD patients.<sup>28</sup> E2F1 enhances EMT by modulating ZEB2 gene expression in SCLC.<sup>29</sup> Our results suggest that E2F proteins are important regulators of BCCIP and E2F transcription factors may play different roles. Further studies are needed to test their complicated contribution in human cancer.

Our study uncovered multiple miRNAs which regulate BCCIP co-expression genes, including miR-484, miR-19A, miR-19B, miR-130a, and miR-130b. Certain miRNAs have been connected with tumor proliferation, cell cycle, apoptosis, infiltration, as well as metastasis. MiR-484 inhibited Apaf-1 which has been linked to the suppression of apoptosis and promotes NSCLC progression.<sup>30</sup> Elevated serum miR-484 expression has been reported to be related to diagnosis, as well as prognosis, in NSCLC patients.<sup>31</sup> In NSCLC cells, miR-19 promotes cell proliferation via inhibiting CBX7 expression and triggers epithelial-mesenchymal transition accompanied by growth inhibition.<sup>32</sup> MiR-130 is markedly linked to the growth, as well as apoptosis of NSCLC cells by targeting PTEN.<sup>33</sup> Upregulation of these miRNAs is consistent with the phenotype of BCCIP excessive expression in LUAD.

To inspect the signaling in controlling BCCIP expression, we performed functional and pathway enrichment analysis for the BCCIP co-expression network. At the same time, GSEA analysis was performed using 475 LUAD samples from TCGA database. DNA repair, cell cycle and the E2F transcription factor family appeared both in enrichment and GSEA analysis. Bioinformatic analysis and WB confirmed that BCCIP was highly correlated with CDK1, FOXM1, CCNB1, and E2F6 which are the key molecules of DNA repair, cell cycle and E2F transcription factor family. Dysregulated DNA repair and cell proliferation controls are motivating factors in tumorigenesis. The E2F transcription factor family plays an important role in lung cancer. These data are consistent with the molecular cascades implicated in LUAD.

The tumor microenvironment is a complicated condition of noncancerous cells primarily constituting immune cells adjacent to tumor cells. In this study, GSEA inspections revealed that low expression samples of BCCIP were enriched in immune cell activation and differentiation. Further, BCCIP expression had a remarkably positive

relationship with tumor purity and a negative relationship with the invasion level of B cells, macrophages, CD4+ T cells, DC and neutrophils in LUAD. Our data provide a profound characterization of the relationship linking BCCIP and immune marker sets in LUAD patients. So far, there is no research to study the relationship between BCCIP and immune cell. Future research with a greater resolution, for instance, with the utilization of single cell RNA sequencing, should be conducted.

In summary, this is the first report on the relationship between BCCIP and LUAD. Higher levels of BCCIP were observed in LUAD, which is correlated with poor prognosis. In vitro, BCCIP promotes LUAD cell proliferation and migration. Herein, we provide multilevel support for the molecular mechanisms of BCCIP in LUAD. Upregulated BCCIP in LUAD may possibly have obvious impacts on DNA repair, cell cycle and the E2F transcription factor family. In addition, our data suggest the prospective novel immune modulatory role of BCCIP in tumor immunity. This study also has limitations. First, there were only 52 LUAD samples to verify the BCCIP expression; more samples are needed to verify the results of our study. Second, the molecular mechanisms underlying why the elevated mRNA level of BCCIP influences DNA repair and cell cycle are still unknown. Additional studies are required to verify this observation.

## ACKNOWLEDGMENTS

We would like to thank the patients enrolled in this study. This work was supported by National Natural Science Foundation of China (No. 81672300) and the project of the free exploration and innovation project of Xi'an Jiaotong University (NO.xjj2018144).

## CONFLICT OF INTEREST

The authors declare that the research was conducted in the absence of any commercial or financial relationships that could be construed as a potential conflict of interest.

## ORCID

Jie Shi  <https://orcid.org/0000-0001-6072-7031>

Wei Li  <https://orcid.org/0000-0003-3258-7662>

## REFERENCES

1. Sung H, Ferlay J, Siegel RL, Laversanne M, Soerjomataram I, Jemal A, et al. Global cancer statistics 2020: GLOBOCAN estimates of incidence and mortality worldwide for 36 cancers in 185 countries. *CA Cancer J Clin.* 2021;71:209–49.
2. Miller KD, Siegel RL, Lin CC, Mariotto AB, Kramer JL, Rowland JH. Cancer treatment and survivorship statistics, 2016. *CA Cancer J Clin.* 2016;66:271–89.
3. Rosenzweig KE, Gomez JE. Concurrent chemotherapy and radiation therapy for inoperable locally advanced non-small-cell lung cancer. *J Clin Oncol.* 2017;35:6–10.
4. Liu J, Yuan Y, Huan J, Shen Z. Inhibition of breast and brain cancer cell growth by BCCIPalpha, an evolutionarily conserved nuclear protein that interacts with BRCA2. *Oncogene.* 2001;20:336–45.
5. Meng X, Liu J, Shen Z. Genomic structure of the human BCCIP gene and its expression in cancer. *Gene.* 2003;302:139–46.

6. Lu H, Guo X, Meng X, Liu J, Allen C, Wray J. The BRCA2-interacting protein BCCIP functions in RAD51 and BRCA2 focus formation and homologous recombinational repair. *Mol Cell Biol* 2005; 25: 1949–1957.
7. Kelso AA, Goodson SD, Watts LE, Ledford LL, Waldvogel SM, Diehl JN. The beta-isoform of BCCIP promotes ADP release from the RAD51 presynaptic filament and enhances homologous DNA pairing. *Nucleic Acids Res.* 2017;45:711–25.
8. Meng X, Yue J, Liu Z, Shen Z. Abrogation of the transactivation activity of p53 by BCCIP down-regulation. *J Biol Chem.* 2007;282:1570–6.
9. Meng X, Fan J, Shen Z. Roles of BCCIP in chromosome stability and cytokinesis. *Oncogene.* 2007;26:6253–60.
10. Fan J, Wray J, Meng X, Shen Z. BCCIP is required for the nuclear localization of the p21 protein. *Cell Cycle.* 2009;8:3019–24.
11. Huhn SC, Liu J, Ye C, Lu H, Jiang X, Feng X. Regulation of spindle integrity and mitotic fidelity by BCCIP. *Oncogene.* 2017; 36:4750–66.
12. Ting YH, Lu TJ, Johnson AW, Shie JT, Chen BR, Kumar SS. Bcp1 is the nuclear chaperone of Rpl23 in *Saccharomyces cerevisiae*. *J Biol Chem.* 2017;292:585–96.
13. Huang YY, Dai L, Gaines D, Droz-Rosario R, Lu H, Liu J. BCCIP suppresses tumor initiation but is required for tumor progression. *Cancer Res.* 2013;73:7122–33.
14. Lu H, Ye C, Feng X, Liu J, Bhaumik M, Xia B. Spontaneous development of hepatocellular carcinoma and B-cell lymphoma in mosaic and heterozygous *Bra2* and *Cdkn1a* interacting protein (*Bccip*) knockout mice. *Am J Pathol.* 2020;190:1175–87.
15. Liu X, Cao L, Ni J, Liu N, Zhao X, Wang Y. Differential BCCIP gene expression in primary human ovarian cancer, renal cell carcinoma and colorectal cancer tissues. *Int J Oncol.* 2013;43:1925–34.
16. Chen L, Ni S, Li M, Shen C, Lin Z, Ouyang Y. High expression of BCCIP beta can promote proliferation of esophageal squamous cell carcinoma. *Dig Dis Sci.* 2017;62:387–95.
17. Cai L, Lin S, Girard L, Zhou Y, Yang L, Ci B. LCE: an open web portal to explore gene expression and clinical associations in lung cancer. *Oncogene.* 2019;38:2551–64.
18. Tang Z, Li C, Kang B, Gao G, Li C, Zhang Z. GEPIA: a web server for cancer and normal gene expression profiling and interactive analyses. *Nucleic Acids Res.* 2017;45(W1):W98–W102.
19. Vasaike SV, Straub P, Wang J, Zhang B. LinkedOmics: analyzing multi-omics data within and across 32 cancer types. *Nucleic Acids Res.* 2018;46(D1):D956–63.
20. Liao Y, Wang J, Jaehnig EJ, Shi Z, Zhang B. WebGestalt 2019: gene set analysis toolkit with revamped UIs and APIs. *Nucleic Acids Res.* 2019; 47(W1):W199–205.
21. Li T, Fan J, Wang B, Traugh N, Chen Q, Liu JS. TIMER: a web server for comprehensive analysis of tumor-infiltrating immune cells. *Cancer Res.* 2017;77:e108–10.
22. Li B, Severson E, Pignon JC, Zhao H, Li T, Novak J. Comprehensive analyses of tumor immunity: implications for cancer immunotherapy. *Genome Biol.* 2016;17:174.
23. Fu Q, Cash SE, Andersen JJ, Kennedy CR, Oldenburg DG, Zander VB. CD43 in the nucleus and cytoplasm of lung cancer is a potential therapeutic target. *Int J Cancer.* 2013;132:1761–70.
24. Wang Q, Su L, Liu N, Zhang L, Xu W, Fang H. Cyclin dependent kinase 1 inhibitors: a review of recent progress. *Curr Med Chem.* 2011;18:2025–43.
25. Shi YX, Zhu T, Zou T, Zhuo W, Chen YX, Huang MS. Prognostic and predictive values of CDK1 and MAD2L1 in lung adenocarcinoma. *Oncotarget.* 2016;7:85235–43.
26. Bradbury A, Hall S, Curtin N, Drew Y. Targeting ATR as cancer therapy: a new era for synthetic lethality and synergistic combinations? *Pharmacol Ther.* 2020;207:107450.
27. Garcia IA, Garro C, Fernandez E, Soria G. Therapeutic opportunities for PLK1 inhibitors: spotlight on BRCA1-deficiency and triple negative breast cancers. *Mutat Res.* 2020;821:111693.
28. Sun CC, Zhou Q, Hu W, Li SJ, Zhang F, Chen ZL. Transcriptional E2F1/2/5/8 as potential targets and transcriptional E2F3/6/7 as new biomarkers for the prognosis of human lung carcinoma. *Aging.* 2018; 10:973–87.
29. Wang T, Chen X, Qiao W, Kong L, Sun D, Li Z. Transcription factor E2F1 promotes EMT by regulating ZEB2 in small cell lung cancer. *BMC Cancer.* 2017;17:719.
30. Li T, Ding ZL, Zheng YL, Wang W. MiR-484 promotes non-small-cell lung cancer (NSCLC) progression through inhibiting Apaf-1 associated with the suppression of apoptosis. *Biomed Pharmacother.* 2017; 96:153–64.
31. Zhuang Z, Sun C, Gong H. High serum miR-484 expression is associated with the diagnosis and prognosis of patients with non-small cell lung cancer. *Exp Ther Med.* 2019;18:4095–102.
32. Peng X, Guan L, Gao B. miRNA-19 promotes non-small-cell lung cancer cell proliferation via inhibiting CBX7 expression. *Onco Targets Ther.* 2018;11:8865–74.
33. Ye L, Wang Y, Nie L, Qian S, Xu M. MiR-130 exerts tumor suppressive function on the tumorigenesis of human non-small cell lung cancer by targeting PTEN. *Am J Transl Res.* 2017;9:1856–65.

## SUPPORTING INFORMATION

Additional supporting information may be found online in the Supporting Information section at the end of this article.

**How to cite this article:** Shi J, Lv X, Li W, Ming Z, Zeng L, Yuan J, et al. Overexpression of BCCIP predicts an unfavorable prognosis and promotes the proliferation and migration of lung adenocarcinoma. *Thorac Cancer.* 2021;12:2324–38. <https://doi.org/10.1111/1759-7714.14073>